MINIGPT-V2: LARGE LANGUAGE MODEL AS A UNIFIED INTERFACE FOR VISION-LANGUAGE MULTI-TASK LEARNING

Jun Chen[1,2*] **Deyao Zhu**[1] **Xiaoqian Shen**[1] **Xiang Li**[1] **Zechun Liu**[2] **Pengchuan Zhang**[2]
Raghuraman Krishnamoorthi[2] **Vikas Chandra**[2] **Yunyang Xiong**[2†] **Mohamed Elhoseiny**[1†]
[1]King Abdullah University of Science and Technology (KAUST)
[2]Meta AI Research

ABSTRACT

Large language models have shown their remarkable capabilities as a general interface for various language-related applications. Motivated by this, we target to build a unified interface for completing many vision-language tasks including image description, visual question answering, and visual grounding, among others. The challenge is to use a single model for performing diverse vision-language tasks effectively with simple multi-modal instructions. Towards this objective, we introduce MiniGPT-v2, a model that can be treated as a unified interface for better handling various vision-language tasks. We propose using unique identifiers for different tasks when training the model. These identifiers enable our model to better distinguish each task instruction effortlessly and also improve the model learning efficiency for each task. After the three-stage training, the experimental results show that MiniGPT-v2 achieves strong performance on many visual question-answering and visual grounding benchmarks compared to other vision-language generalist models. Our model and codes are available at `https://minigpt-v2.github.io/`.

1 INTRODUCTION

Multi-modal Large Language Models (LLMs) have emerged as an exciting research topic with a rich set of applications in vision-language community, such as visual AI assistant, image captioning, visual question answering (VQA), and referring expression comprehension (REC). A key feature of multimodal large language models is that they can inherit advanced capabilities (e.g., logical reasoning, common sense, and strong language expression) from the LLMs (OpenAI, 2022; Touvron et al., 2023a;b; Chiang et al., 2023). When tuned with proper vision-language instructions, multi-modal LLMs, specifically vision-language models, demonstrate strong capabilities such as producing detailed image descriptions, generating code, localizing the visual objects in the image, and even performing multi-modal reasoning to better answer complicated visual questions (Zhu et al., 2023b; Liu et al., 2023b; Ye et al., 2023; Wang et al., 2023; Chen et al., 2023b; Dai et al., 2023; Zhu et al., 2023a; Chen et al., 2023a; Zhuge et al., 2023). This evolution of LLMs enables interactions of visual and language inputs across communication with individuals and has been shown quite effective for building visual chatbots.

However, learning to perform multiple vision-language tasks effectively and formulating their corresponding multi-modal instructions present considerable challenges due to the complexities inherent among different tasks. For instance, given a user input *"tell me the location of a person"*, there are many ways to interpret and respond based on the specific task. In the context of the referring expression comprehension task, it can be answered with one bounding box location of the person. For the visual question-answering task, the model might describe their spatial location using human natural language. For the person detection task, the model might identify every spatial location of each human in a given image. To alleviate this issue and towards a unified approach, we propose

[*]Work partially done during the internship at Meta AI
[†]Equal last author

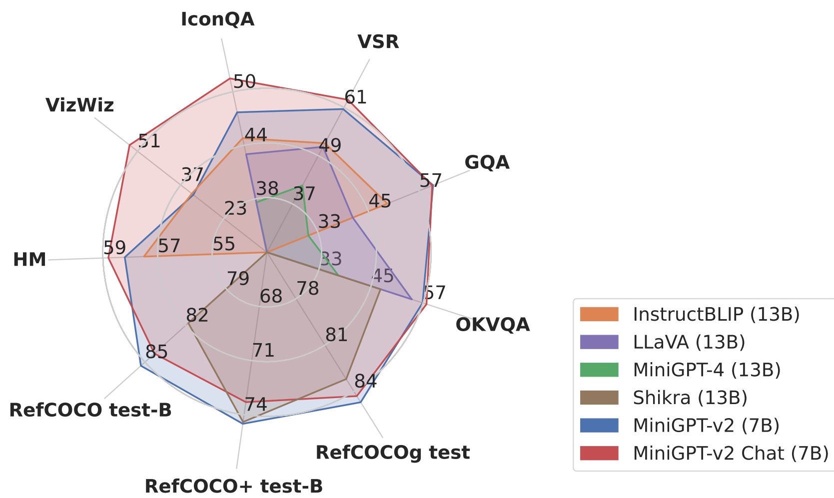

Figure 1: Our MiniGPT-v2 achieves state-of-the-art performances on a broad range of vision-language tasks compared with other generalist models.

a task-oriented instruction training scheme to reduce the multi-modal instructional ambiguity, and a vision-language model, MiniGPT-v2. Specifically, we provide a unique task identifier token for each task. For example, we provide a *[vqa]* identifier token for training all the data samples from the visual question answering tasks. In total, we provide six different task identifiers during the model training stages.

Our model, MiniGPT-v2, has a simple architecture design. It directly takes the visual tokens from a ViT vision encoder (Fang et al., 2022) and project them into the feature space of a large language model (Touvron et al., 2023b). For better visual perception, we utilize higher-resolution images (448x448) during training. But this will result in a larger number of visual tokens. To make the model training more efficient, we concatenate every four neighboring visual tokens into a single token, reducing the total number by 75%. Additionally, we utilize a three-stage training strategy to effectively train our model with a mixture of weakly-labeled, fine-grained image-text datasets, and multi-modal instructional datasets, with different training focus at each stage.

To evaluate the performance of our model, we conducted extensive experiments on diverse vision-language tasks, including (detailed) image/grounded captioning, vision question answering, and visual grounding. The results demonstrate that our MiniGPT-v2 can achieve SOTA or comparable performance on diverse benchmarks compared to previous vision-language generalist models, such as MiniGPT-4 (Zhu et al., 2023b), InstructBLIP (Dai et al., 2023), LLaVA (Liu et al., 2023b) and Shikra (Chen et al., 2023b). For example, our MiniGPT-v2 outperforms MiniGPT-4 by 21.3%, InstructBLIP by 11.3%, and LLaVA by 11.7% on the VSR benchmark (Liu et al., 2023a), and it also performs better than the previously established strong baseline, Shikra, in most validations on RefCOCO, RefCOCO+, and RefCOCOg. Our model establishes new state-of-the-art results on these benchmarks among vision-language generalist models, shown in Fig. 1.

2 RELATED WORK

We briefly review relevant works on advanced large language models and multi-modal LLMs for visual aligning.

Advanced Large Language Models (LLMs). Early-stage models such as GPT-2 (Radford et al., 2019) and BERT (Devlin et al., 2018) are foundation models trained on web-scale text datasets, marking a breakthrough in the NLP field. Following the success of foundation models, LLMs with higher capacity and increased training data are developed, including GPT-3 (Brown et al., 2020), Megatron-turing NLG (Smith et al., 2022), PaLM (Chowdhery et al., 2022), Gopher (Rae et al., 2021), Chinchilla (Hoffmann et al., 2022), OPT (Zhang et al., 2022), and BLOOM (Scao et al., 2022). Most recently, the efforts have been focused on refining LLMs to work effectively with human instruction and feedback. Representative works in this direction are InstructGPT (Ouyang et al., 2022) and ChatGPT (OpenAI, 2022), which demonstrate strong capabilities such as answering a diverse range of language questions, engaging in conversations with humans, and learning to perform complex tasks like writing refinement and coding assistant.

Concurrent with these advancements of LLMs is the rise of LLaMA (Touvron et al., 2023a) language models. To enable human instruction following abilities similar to ChatGPT, some works attempt to finetune the LLaMA model with additional high-quality instruction datasets (sha, 2023). Examples of these models include Alpaca (Taori et al., 2023), Vicuna (Chiang et al., 2023), and MPT (Team, 2023). Some other open-sourced language models that learned from the human feedback data, such as Falcon (Penedo et al., 2023) and LLaMA-2 (Touvron et al., 2023b), have also been introduced to the NLP community with impressive performance.

Visual Aligning with LLMs. With the remarkable generalization abilities of LLMs, interesting studies have extended LLMs to multi-modal domains by aligning visual inputs with LLMs. Early works such as VisualGPT (Chen et al., 2022) and Frozen (Tsimpoukelli et al., 2021) used pre-trained language models to improve vision-language models on image captioning and visual question answering. This initial exploration paved the way for subsequent vision-language research such as Flamingo (Alayrac et al., 2022) and BLIP-2 (Li et al., 2023a). More recently, GPT-4 has been released and demonstrates many advanced multi-modal abilities, e.g., generating website code based on handwritten text instructions. Those demonstrated capabilities inspired other vision-language LLMs, including MiniGPT-4 (Zhu et al., 2023b) and LLaVA (Liu et al., 2023b), which align the image inputs with a large language model, Vicuna Chiang et al. (2023), using proper instructional tuning. These vision-language models also showcase many advanced multi-modal capabilities after the alignment. Recent works, such as Vision-LLM (Wang et al., 2023), Kosmos-2 (Peng et al., 2023), Shikra (Chen et al., 2023b), and our concurrent work, Qwen-VL (Bai et al., 2023), also demonstrate that multi-model LLMs models can also perform visual grounding by generating the text format of bounding boxes through language model.

3 METHOD

We start by introducing our vision-language model, MiniGPT-v2, then discuss the basic idea of a multi-task instruction template with task identifiers for training, and finally adapt our task identifier idea to achieve task-oriented instruction tuning.

3.1 MODEL ARCHITECTURE

Our proposed model architecture, MiniGPT-v2, is shown in Fig. 2. It consists of three components: a visual backbone, a linear projection layer, and a large language model. We describe each component as follows:

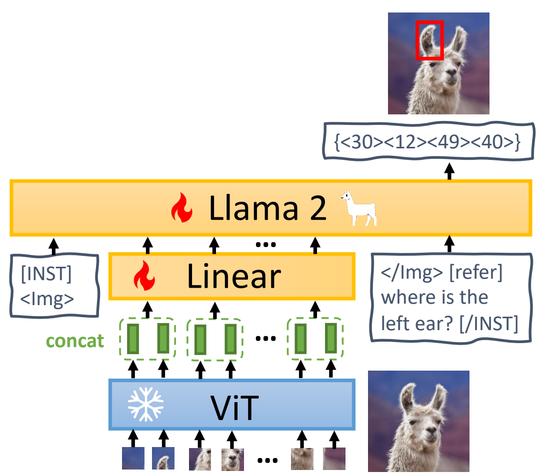

Figure 2: **Architecture of MiniGPT-v2.** The model takes a ViT visual backbone, which remains frozen during all training phases. We concatenate four adjacent visual output tokens from ViT backbone and project them into LLaMA-2 language model space via a linear projection layer.

Visual backbone. MiniGPT-v2 adapts the EVA (Fang et al., 2022) as our visual backbone model backbone. We freeze the visual backbone during the entire model training. We train our model with the image resolution 448x448, and we interpolate the positional encoding to scale with a higher image resolution.

Linear projection layer. We aim to project all the visual tokens from the frozen vision backbone into the language model space. However, for higher-resolution images such as 448x448, projecting all the image tokens results in a very long-sequence input (e.g., 1024 tokens) and significantly lowers the training and inference efficiency. Hence, we simply concatenate 4 adjacent visual tokens in the embedding space and project them together into one single embedding in the same feature space of the large language model, thus reducing the number of visual input tokens by 4 times. With this operation, our MiniGPT-v2 can process high-resolution images much more efficiently during the training and inference stage.

Large language model. MiniGPT-v2 adopts the open-sourced LLaMA2-chat (7B) (Touvron et al., 2023b) as the language model backbone. In our work, the language model is treated as a unified interface for various vision-language inputs. We directly rely on the LLaMA-2 language tokens to perform various vision-language tasks. For the visual grounding tasks that necessitate the generation of spatial locations, we directly ask the language model to produce textual representations of bounding boxes to denote their spatial positions.

3.2 Multi-task Instruction Template

When training a single unified model for multiple different tasks such as visual question answering, image caption, referring expression, grounded image caption, and region identification, the multi-modal model might fail to distinguish each task by just aligning visual tokens to language models. For instance, when you ask "Tell me the spatial location of the person wearing a red jacket?", the model can either respond you the location in a bounding box format (e.g., $< \mathrm{X}_{left} >< \mathrm{Y}_{top} >< \mathrm{X}_{right} >< \mathrm{Y}_{bottom} >$) or describe the object location using natural language (e.g., upper right corner). To reduce such ambiguity and make each task easily distinguishable, we introduce task-specific tokens in our designed multi-task instruction template for training. We now describe our multi-task instruction template in more details.

General input format. We follow the LLaMA-2 conversation template design and adapt it for the multi-modal instructional template. The template is denoted as follows,

[INST] <Img> < ImageFeature> </Img> [Task Identifier] Instruction [/INST]

In this template, *[INST]* is considered as the user role, and *[/INST]* is considered as the assistant role. We structure the user input into three parts. The first part is the image features, the second part is the task identifier token, and the third part is the instruction input.

Task identifier tokens. Our model takes a distinct identifier for each task to reduce the ambiguity across various tasks. As illustrated in Table 1, we have proposed six different task identifiers for visual question answering, image caption, grounded image captioning, referring expression comprehension, referring expression generation, and phrase parsing and grounding respectively. For vision-irrelevant instructions, our model does not use any task identifier token.

Tasks	VQA	Caption	Grounded Caption	REC	REG	Object Parsing and Grounding
Identifiers	[vqa]	[caption]	[grounding]	[refer]	[identify]	[detection]

Table 1: Task identifier tokens for 6 different tasks, including visual question answering, image captioning, grounded image captioning, referring expression comprehension (REC), referring expression generation (REG), and object parsing and grounding (where the model extracts objects from the input text and determines their bounding box locations).

Spatial location representation. For tasks such as referring expression comprehension (REC), referring expression generation (REG), and grounded image captioning, our model is required to identify the spatial location of the referred objects accurately. We represent the spatial location through the textual formatting of bounding boxes in our setting, specifically: "$\{< \mathrm{X}_{left} >< \mathrm{Y}_{top} >< \mathrm{X}_{right} >< \mathrm{Y}_{bottom} >\}$". Coordinates for X and Y are represented by integer values normalized in the range [0,100]. $< \mathrm{X}_{left} >$ and $< \mathrm{Y}_{top} >$ denote the x and y coordinate top-left corner of the generated bounding box, and $< \mathrm{X}_{right} >$ and $< \mathrm{Y}_{bottom} >$ denote the x and y coordinates of the bottom-right corner.

3.3 Multi-task Instruction Training

We now adapt our designed multi-task instruction template for instruction training. The basic idea is to take instruction with task-specific identifier token as input for task-oriented instruction training of MiniGPT-v2. When input instructions have task identifier tokens, our model will become more prone to multiple-task understanding during training. We train our model with task identifier instructions for better visual aligment in three stages. The first stage is to help MiniGPT-v2 build broad vision-language knowledge through many weakly-labeled image-text datasets, and high-quality fine-grained vision-language annotation datasets as well (where we will assign a high data sampling ratio for weakly-labeled image-text datasets). The second stage is to improve the model with only fine-grained data for multiple tasks. The third stage is to finetune our model with more multi-modal instruction and language datasets for answering diverse multi-modal instructions better and behaving as a multi-modal chatbot. The datasets used for training at each stage are listed in Table 2.

Data types	Dataset	Stage 1	Stage 2	Stage 3
Weakly-labeled	GRIT-20M (REC and REG), LAION, CC3M, SBU	✓	✗	✗
Grounded caption	GRIT-20M	✓	✗	✗
Caption	COCO caption, Text Captions	✓	✓	✓
REC	RefCOCO, RefCOCO+, RefCOCOg, Visual Genome	✓	✓	✓
REG	RefCOCO, RefCOCO+, RefCOCOg	✓	✓	✓
VQA	GQA, VQAv2, OCR-VQA, OK-VQA, AOK-VQA	✓	✓	✓
Multimodal instruction	LLaVA dataset, Flickr30k, Multi-task conversation	✗	✗	✓
Langauge dataset	Unnatural Instructions	✗	✗	✓

Table 2: The training datasets used for our model three-stage training.

Stage 1: Pretraining. To have broad vision-language knowledge, our model is trained on a mix of weakly-labeled and fine-grained datasets. We give a high sampling ratio for weakly-labeled datasets to gain more diverse knowledge in the first-stage.

For the weakly-labeled datasets, we use LAION (Schuhmann et al., 2021), CC3M (Sharma et al., 2018), SBU (Ordonez et al., 2011), and GRIT-20M from Kosmos v2 (Peng et al., 2023) that built the dataset for referring expression comprehension (REC), referring expression generation (REG), and grounded image captioning.

For fine-grained datasets, we use datasets like COCO caption (Lin et al., 2014) and Text Captions (Sidorov et al., 2020) for image captioning, RefCOCO (Kazemzadeh et al., 2014), RefCOCO+ (Yu et al., 2016), and RefCOCOg (Mao et al., 2016) for REC. For REG, we restructured the data from ReferCOCO and its variants, reversing the order from phrase $\rightarrow$ bounding boxes to bounding boxes $\rightarrow$ phrase. For VQA datasets, our training takes a variety of datasets, such as GQA (Hudson & Manning, 2019), VQA-v2 (Goyal et al., 2017), OCR-VQA (Mishra et al., 2019), OK-VQA (Marino et al., 2019), and AOK-VQA (Schwenk et al., 2022).

Stage 2: Multi-task training. To improve the performance of MiniGPT-v2 on each task, we only focus on using fine-grained datasets to train our model at this stage. We exclude the weakly-supervised datasets such as GRIT-20M and LAION from stage-1 and update the data sampling ratio according to the frequency of each task. This strategy enables our model to prioritize high-quality aligned image-text data for superior performance across various tasks.

Stage 3: Multi-modal instruction tuning. Subsequently, we focus on tuning our model with more multi-modal instruction datasets and enhancing its conversation ability as a chatbot. We continue using the datasets from the second stage and add instructional datasets, including LLaVA (Liu et al., 2023b), Flickr30k dataset (Plummer et al., 2015), our constructed mixing multi-task dataset, and the language dataset, Unnatural Instruction (Honovich et al., 2022). We give a lower data sampling ratio for the fine-grained datasets from stage-2 and a higher data sampling ratio for the new instruction datasets.

– LLaVA instruction data. We add the multi-modal instruction tuning datasets, including the detailed descriptions and complex reasoning from LLaVA (Liu et al., 2023b), with 23k and 58k data examples respectively.

– Flicker 30k. After the second-stage training, our MiniGPT-v2 can effectively generate the grounded image caption. Nevertheless, these descriptions tend to be short and often cover very few number of visual objects. This is because the GRIT-20M dataset from KOSMOS-v2 (Peng et al., 2023) that our model was trained with, features a limited number of grounded visual objects in each caption, and our model lacks proper multi-modal instruction tuning to teach it to recognize more visual objects. To improve this, we fine-tune our model using the Flickr30k dataset (Plummer et al., 2015), which provides more contextual grounding of entities within its captions.

We prepare the Flickr30k dataset in two distinct formats for training our model to perform grounded image caption and a new task "object parsing and grounding":

1) **Grounded image caption.** We select captions with a minimum of five grounded phrases, containing around 2.5k samples, and we directly instruct the model to produce the grounded image caption. e.g., *a <p>wooden table</p>*$\{<X_{left}><Y_{top}><X_{right}><Y_{bottom}>\}$ *in the center of the room.*

2) **Object parsing and grounding.** This new task is to parse all the objects from an input caption and then ground each object. To enable this, we use the task identifier*[detection]* to differentiate this capability from other tasks. Also, we use Flickr30k to construct two types of instruction datasets: caption$\rightarrow$ grounded phrases and phrase $\rightarrow$ grounded phrase, each containing around 2.5k and 3k samples. Then we prompt our model with the instruction: *[detection] description*, the model will directly parse the objects from the input image description and also ground the objects into bounding boxes.

– Mixing multi-task dataset. After extensive training with single-round instruction-answer pairs, the model might not handle multiple tasks well during multi-round conversations since the context becomes more complex. To alleviate this situation, we create a new multi-round conversation dataset by mixing the data from different tasks. We include this dataset into our third-stage model training.

– Unnatural instruction. The conversation abilities of language model can be reduced after extensive vision-language training. To fix this, we add the language dataset, Unnatural Instruction (Honovich et al., 2022) into our model's third-stage training for helping recover the language generation ability.

4 EXPERIMENTS

In this section, we present experimental settings and results. We primarily conduct experiments on (detailed) image/grounded captioning, vision question answering, and visual grounding tasks, including referring expression comprehension. We present both quantitative and qualitative results.

Implementation details. Throughout the entire training process, the visual backbone of MiniGPT-v2 remains frozen. We focus on training the linear projection layer and efficient finetuning the language model using LoRA (Hu et al., 2021). With LoRA, we finetune $\mathcal{W}_q$ and $\mathcal{W}_v$ via low-rank adaptation. In our implementation, we set the rank, $r = 64$. We trained the model with an image resolution of 448x448 during all stages. During each stage, we use our designed multi-modal instructional templates for various vision-language tasks during the model training.

Training and hyperparameters. We use AdamW optimizer with a cosine learning rate scheduler to train our model. In the initial stage, we train on 8xA100 GPUs for 400,000 steps with a global batch size of 96 and an maximum learning rate of 1e-4. This stage takes around 90 hours. During the second stage, the model is trained for 50,000 steps on 4xA100 GPUs with a maximum learning rate of 1e-5, adopting a global batch size of 64, and this training stage lasts roughly 20 hours. For the last stage, training is executed for another 35,000 steps on 4xA100 GPUs, using a global batch size of 24 and this training stage took around 7 hours, maintaining the same maximum learning rate of 1e-5.

4.1 QUANTITATIVE EVALUATION

Dataset and evaluation metrics. We evaluate our model across a range of VQA and visual grounding benchmarks. For VQA benchmarks, we consider OKVQA (Schwenk et al., 2022), GQA (Hudson & Manning, 2019), visual spatial reasoning (VSR) (Liu et al., 2023a), IconVQA (Lu et al., 2021), VizWiz (Gurari et al., 2018), HatefulMemes (HM) (Kiela et al., 2020), and TextVQA (Singh et al., 2019). For visual grounding, we evaluate our model on RefCOCO (Kazemzadeh et al., 2014) and RefCOCO+(Yu et al., 2016), and RefCOCOg(Mao et al., 2016) benchmarks.

To evaluate VQA benchmarks, we use an open-ended approach with a greedy decoding strategy. We evaluate each VQA question with the following instruction template: *"[vqa] question"*. Following the previous method (Dai et al., 2023), we evaluate the performance by matching the model's

Method	Grounding	OKVQA	GQA	VSR (zero-shot)	IconVQA (zero-shot)	VizWiz (zero-shot)	HM (zero-shot)
Flamingo-9B	✗	44.7	-	31.8	-	28.8	57.0
BLIP-2 (13B)	✗	45.9	41.0	50.9	40.6	19.6	53.7
InstructBLIP (13B)	✗	-	49.5	52.1	44.8	33.4	57.5
MiniGPT-4 (13B)	✗	37.5	30.8	41.6	37.6	-	-
LLaVA (13B)	✗	54.4	41.3	51.2	43.0	-	-
Shikra (13B)	✓	47.2	-	-	-	-	-
Ours (7B)	✓	56.9	**60.3**	60.6	47.7	32.9	58.2
Ours (7B)-chat	✓	**57.8**	60.1	**62.9**	**51.5**	**53.6**	**58.8**

Table 3: **Results on multiple VQA tasks.** We report top-1 accuracy for each task. Grounding column indicates whether the model incorporates visual localization capability. The best performance for each benchmark is indicated in **bold**.

Method	Model types	RefCOCO			RefCOCO+			RefCOCOg		Avg
		val	test-A	test-B	val	test-A	test-B	val	test	
UNINEXT	Specialist models	92.64	94.33	91.46	85.24	89.63	79.79	88.73	89.37	88.90
G-DINO-L	Specialist models	90.56	93.19	88.24	82.75	88.95	75.92	86.13	87.02	86.60
VisionLLM-H	Generalist models	-	86.70	-	-	-	-	-	-	-
OFA-L	Generalist models	79.96	83.67	76.39	68.29	76.00	61.75	67.57	67.58	72.65
Shikra (7B)	Generalist models	87.01	90.61	80.24	81.60	87.36	72.12	82.27	82.19	82.93
Shikra (13B)	Generalist models	87.83	91.11	81.81	**82.89**	**87.79**	74.41	82.64	83.16	83.96
Ours (7B)	Generalist models	**88.69**	**91.65**	**85.33**	79.97	85.12	**74.45**	**84.44**	**84.66**	**84.29**
Ours (7B)-chat	Generalist models	88.06	91.29	84.30	79.58	85.52	73.32	84.19	84.31	83.70

Table 4: **Results on referring expression comprehension tasks.** Our MiniGPT-v2 outperforms many VL-generalist models including VisionLLM (Wang et al., 2023), OFA (Wang et al., 2022) and Shikra (Chen et al., 2023b) and reduces the accuracy gap comparing to specialist models including UNINEXT (Yan et al., 2023) and G-DINO (Liu et al., 2023c).

response to the ground-truth and reporting top-1 accuracy. For visual grounding benchmarks, we use the template *"[refer] give me the location of Referring expression"* for each referring expression comprehension question, and a predicted bounding box is considered as correct for reporting accuracy if its IOU between prediction and ground-truth is higher than 0.5.

Visual question answering results. Table 3 presents our experimental results on multiple VQA benchmarks. Our results compare favorably to baselines including MiniGPT-4 (Zhu et al., 2023b), Shikra (Chen et al., 2023b), LLaVA (Liu et al., 2023b), and InstructBLIP (Dai et al., 2023) across all the VQA tasks. For example, on QKVQA, our MiniGPT-v2 outperforms MiniGPT-4, Shikra, LLaVA, and BLIP-2 by 20.3%, 10.6%, 3.4%, and 11.9%. These results indicate the strong visual question answering capabilities of our model. Furthermore, we find that our MiniGPT-v2 (chat) variant shows higher performance than the version trained after the second stage. On OKVQA, VSR, IconVQA, VizWiz, and HM, MiniGPT-v2 (chat) outperforms MiniGPT-v2 by 0.9%, 2.3%, 4.2%, 20.7%, and 0.6%. We believe that the better performance can be attributed to the improved language skills during the third-stage training, which is able to benefit visual question comprehension and response, especially on VizWiz with 20.7% top-1 accuracy increase.

Referring expression comprehension results. Table 4 compares our model to baselines on REC benchmarks. Our MiniGPT-v2 shows strong REC performance on RefCOCO, RefCOCO+, and RefCOCOg, performing better than other vision-language generalist models. MiniGPT-v2 outperforms OFA-L (Wang et al., 2022) by over 8% accuracy across all tasks of RefCOCO/RefCOCO+/RefCOCOg. Compared with a strong baseline, Shikra (13B) (Chen et al., 2023b), our model still shows better results, e.g., 84.29% vs 83.96% accuracy in average. These results provide direct evidence for the competing visual grounding capabilities of MiniGPT-v2. Although our model underperforms specialist models, the promising performance indicates its growing competence in visual grounding.

Ablation on task identifier. We conduct ablation studies on the effect of the task identifier on the performance of MiniGPT-v2. We compare our model with the variant without using task iden-

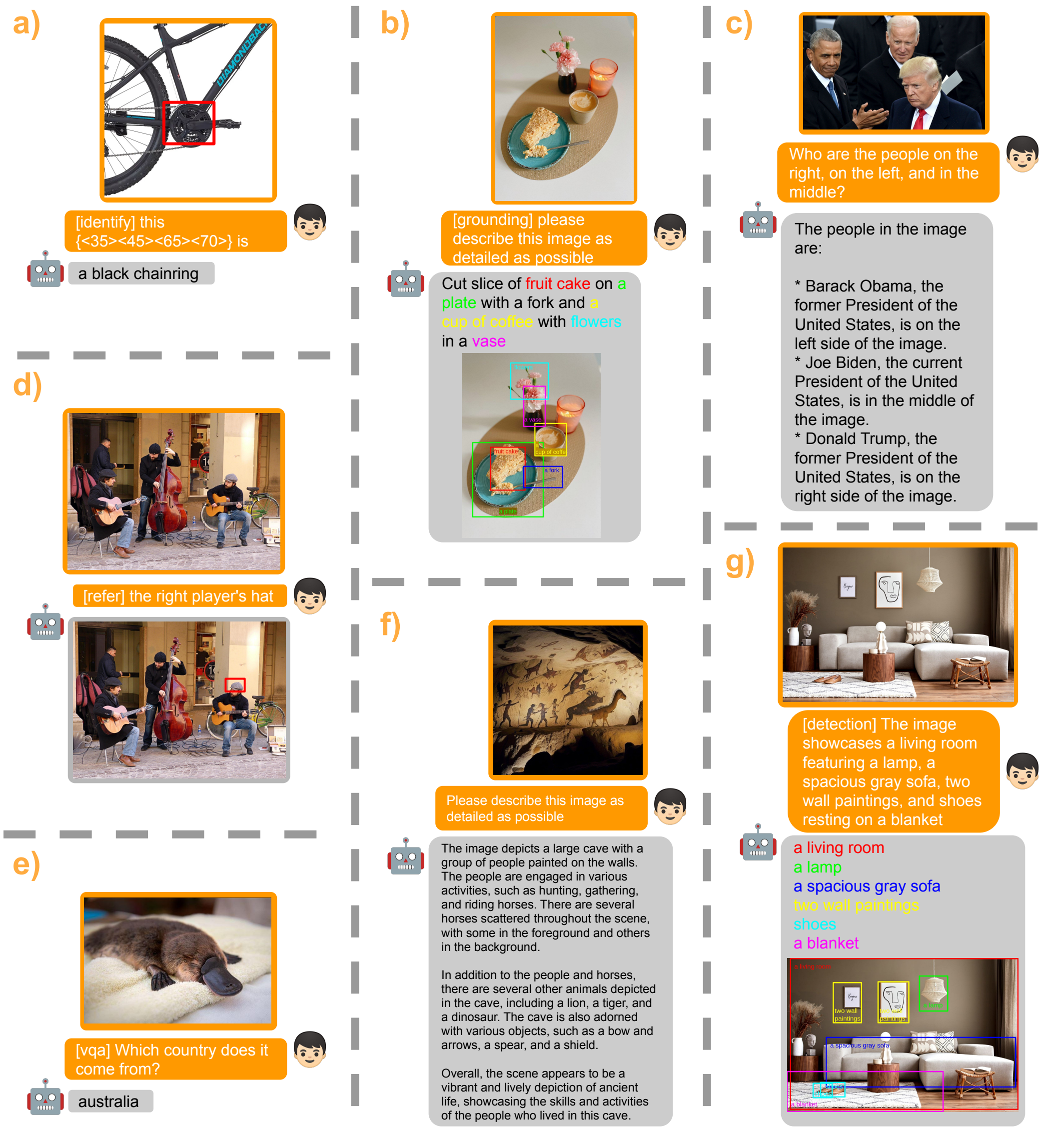

Figure 3: **Examples for various multi-modal capabilities of MiniGPT-v2.** We showcase that our model is capable of completing multiple tasks such as referring expression comprehension, referring expression generation, detailed grounded image caption, visual question answering, detailed image description, and directly parsing phrase and grounding from a given input text.

	OKVQA	GQA	WizViz	VSR	IconVQA	HM	Average
Ours w/o task identifier	50.5	53.4	28.6	57.5	44.8	56.8	48.6
Ours	**52.1**	**54.6**	**29.4**	**59.9**	**45.6**	**57.4**	**49.8**

Table 5: Task identifier ablation study on VQA benchmarks. With task identifier during the model training can overall improve VQA performances from multiple VQA benchmarks

tifiers on VQA benchmarks. Both models were trained on 4xA100 GPUs for 24 hours with an equal number of training steps for multiple vision-language tasks. Results in Table 5 demonstrate the performance on multiple VQA benchmarks and consistently show that token identifier training benefits the overall performance of MiniGPT-v2. Specifically, our MiniGPT-v2 with task-oriented instruction training achieves 1.2% top-1 accuracy improvement on average. These ablation results can validate the clear advantage of adding task identifier tokens and support the use of multi-task identifiers for multi-task learning efficiency.

Hallucination. We measure the hallucination of our model on image description generation and compare the results with other vision-language baselines, including MiniGPT-4 (Zhu et al., 2023b), mPLUG-Owl (Ye et al., 2023), LLaVA (Liu et al., 2023b), and MultiModal-GPT (Gong et al., 2023). Following the methodology from (Li et al., 2023b), we use CHAIR (Rohrbach et al., 2018) to assess hallucination at both object and sentence levels. As shown in Table 6, we find that our MiniGPT-v2 tends to generate the image description with reduced hallucination compared to other baselines. We have evaluated three types of prompts in MiniGPT-v2. First, we use the prompt *generate a brief description of the given image* without any specific task identifier which tends to produce more detailed image descriptions. Then we provide the instruction prompt *[grounding] describe this image in as detailed as possible* for evaluating grounded image captions. Lastly, we prompt our model with *[caption] briefly describe the image*. With these task identifiers, MiniGPT-v2 is able to produce a variety of image descriptions with different levels of hallucination. As a result, all these three instruction variants have lower hallucination than our baseline, especially with the task specifiers of *[caption]* and *[grounding]*.

Method	CHAIR$_I$ ↓	CHAIR$_S$ ↓	Len
MiniGPT-4	9.2	31.5	116.2
mPLUG-Owl	30.2	76.8	98.5
LLaVA	18.8	62.7	90.7
MultiModal-GPT	18.2	36.2	45.7
MiniGPT-v2 (long)	8.7	25.3	56.5
MiniGPT-v2 (grounded)	7.6	12.5	18.9
MiniGPT-v2 (short)	**4.4**	**7.1**	**10.3**

Table 6: **Results on hallucination.** We evaluate the hallucination of MiniGPT-v2 with different instructional templates and output three versions of captions for evaluation. For the “long” version, we use the prompt *generate a brief description of the given image*. For the “grounded” version, the instruction is *[grounding] describe this image in as detailed as possible*. For the “short” version, the prompt is *[caption] briefly describe the image*.

4.2 Qualitative Results

We now provide the qualitative results for a complementary understanding of our model's multimodal capabilities. Some examples can be seen in Fig. 3. Specifically, we demonstrated various abilities in the examples including a) object identification; b) detailed grounded image captioning; c) visual question answering; d) referring expression comprehension; e) visual question answering under task identifier; f) detailed image description; g) object parsing and grounding from an input text. More qualitative results can be found in the Appendix. These results demonstrate that our model has competing vision-language understanding capabilities. Moreover, notice that we train our model only with a few thousand of instruction samples on object parsing and grounding tasks at the third-stage, and our model can effectively follow the instructions and generalize on the new task. This indicates that our model has the flexibility to adapt on many new tasks.

Note that our model still occasionally shows hallucinations when generating the image description or visual grounding. e.g., our model may sometimes produce descriptions of non-existent visual objects or generate inaccurate visual locations of grounded objects. We believe training with more high-quality image-text aligned data and integrating with a stronger vision backbone or large language model hold the potential for alleviating this issue.

5 Conclusion

In this paper, we introduce MiniGPT-v2, a multi-modal LLM that can serve as a unified interface for various vision-language multi-tasking learning. To develop a single model capable of handling multiple vision-language tasks, we propose using distinct identifiers for each task during the training and inference. These identifiers help our model easily differentiate various tasks and also improve learning efficiency. Our MiniGPT-v2 achieves state-of-the-art results across many visual question answering and referring expression comprehension benchmarks. We also found that our model can efficiently adapt to new vision-language tasks, which suggests that MiniGPT-v2 has many potential applications in the vision-language community.

REFERENCES

Sharegpt. https://github.com/domeccleston/sharegpt, 2023.

Jean-Baptiste Alayrac, Jeff Donahue, Pauline Luc, Antoine Miech, Iain Barr, Yana Hasson, Karel Lenc, Arthur Mensch, Katherine Millican, Malcolm Reynolds, et al. Flamingo: a visual language model for few-shot learning. In *Advances in Neural Information Processing Systems*, 2022.

Jinze Bai, Shuai Bai, Shusheng Yang, Shijie Wang, Sinan Tan, Peng Wang, Junyang Lin, Chang Zhou, and Jingren Zhou. Qwen-vl: A frontier large vision-language model with versatile abilities. *arXiv preprint arXiv:2308.12966*, 2023.

Tom Brown, Benjamin Mann, Nick Ryder, Melanie Subbiah, Jared D Kaplan, Prafulla Dhariwal, Arvind Neelakantan, Pranav Shyam, Girish Sastry, Amanda Askell, et al. Language models are few-shot learners. *Advances in neural information processing systems*, 33:1877–1901, 2020.

Jun Chen, Han Guo, Kai Yi, Boyang Li, and Mohamed Elhoseiny. Visualgpt: Data-efficient adaptation of pretrained language models for image captioning. In *Proceedings of the IEEE/CVF Conference on Computer Vision and Pattern Recognition*, pp. 18030–18040, 2022.

Jun Chen, Deyao Zhu, Kilichbek Haydarov, Xiang Li, and Mohamed Elhoseiny. Video chatcaptioner: Towards the enriched spatiotemporal descriptions. *arXiv preprint arXiv:2304.04227*, 2023a.

Keqin Chen, Zhao Zhang, Weili Zeng, Richong Zhang, Feng Zhu, and Rui Zhao. Shikra: Unleashing multimodal llm's referential dialogue magic. *arXiv preprint arXiv:2306.15195*, 2023b.

Wei-Lin Chiang, Zhuohan Li, Zi Lin, Ying Sheng, Zhanghao Wu, Hao Zhang, Lianmin Zheng, Siyuan Zhuang, Yonghao Zhuang, Joseph E. Gonzalez, Ion Stoica, and Eric P. Xing. Vicuna: An open-source chatbot impressing gpt-4 with 90%* chatgpt quality, March 2023. URL https://vicuna.lmsys.org.

Aakanksha Chowdhery, Sharan Narang, Jacob Devlin, Maarten Bosma, Gaurav Mishra, Adam Roberts, Paul Barham, Hyung Won Chung, Charles Sutton, Sebastian Gehrmann, et al. Palm: Scaling language modeling with pathways. *arXiv preprint arXiv:2204.02311*, 2022.

Wenliang Dai, Junnan Li, Dongxu Li, Anthony Meng Huat Tiong, Junqi Zhao, Weisheng Wang, Boyang Li, Pascale Fung, and Steven Hoi. Instructblip: Towards general-purpose vision-language models with instruction tuning, 2023.

Jacob Devlin, Ming-Wei Chang, Kenton Lee, and Kristina Toutanova. Bert: Pre-training of deep bidirectional transformers for language understanding. *arXiv preprint arXiv:1810.04805*, 2018.

Yuxin Fang, Wen Wang, Binhui Xie, Quan Sun, Ledell Wu, Xinggang Wang, Tiejun Huang, Xinlong Wang, and Yue Cao. Eva: Exploring the limits of masked visual representation learning at scale. *arXiv preprint arXiv:2211.07636*, 2022.

Tao Gong, Chengqi Lyu, Shilong Zhang, Yudong Wang, Miao Zheng, Qian Zhao, Kuikun Liu, Wenwei Zhang, Ping Luo, and Kai Chen. Multimodal-gpt: A vision and language model for dialogue with humans. *arXiv preprint arXiv:2305.04790*, 2023.

Yash Goyal, Tejas Khot, Douglas Summers-Stay, Dhruv Batra, and Devi Parikh. Making the v in vqa matter: Elevating the role of image understanding in visual question answering. In *Proceedings of the IEEE conference on computer vision and pattern recognition*, pp. 6904–6913, 2017.

Danna Gurari, Qing Li, Abigale J Stangl, Anhong Guo, Chi Lin, Kristen Grauman, Jiebo Luo, and Jeffrey P Bigham. Vizwiz grand challenge: Answering visual questions from blind people. In *Proceedings of the IEEE conference on computer vision and pattern recognition*, pp. 3608–3617, 2018.

Jordan Hoffmann, Sebastian Borgeaud, Arthur Mensch, Elena Buchatskaya, Trevor Cai, Eliza Rutherford, Diego de Las Casas, Lisa Anne Hendricks, Johannes Welbl, Aidan Clark, et al. Training compute-optimal large language models. *arXiv preprint arXiv:2203.15556*, 2022.

Or Honovich, Thomas Scialom, Omer Levy, and Timo Schick. Unnatural instructions: Tuning language models with (almost) no human labor. *arXiv preprint arXiv:2212.09689*, 2022.

Edward J Hu, Yelong Shen, Phillip Wallis, Zeyuan Allen-Zhu, Yuanzhi Li, Shean Wang, Lu Wang, and Weizhu Chen. Lora: Low-rank adaptation of large language models. *arXiv preprint arXiv:2106.09685*, 2021.

Drew A Hudson and Christopher D Manning. Gqa: A new dataset for real-world visual reasoning and compositional question answering. In *Proceedings of the IEEE/CVF conference on computer vision and pattern recognition*, pp. 6700–6709, 2019.

Sahar Kazemzadeh, Vicente Ordonez, Mark Matten, and Tamara Berg. Referitgame: Referring to objects in photographs of natural scenes. In *Proceedings of the 2014 conference on empirical methods in natural language processing (EMNLP)*, pp. 787–798, 2014.

Douwe Kiela, Hamed Firooz, Aravind Mohan, Vedanuj Goswami, Amanpreet Singh, Pratik Ringshia, and Davide Testuggine. The hateful memes challenge: Detecting hate speech in multimodal memes. *Advances in neural information processing systems*, 33:2611–2624, 2020.

Junnan Li, Dongxu Li, Silvio Savarese, and Steven Hoi. Blip-2: Bootstrapping language-image pre-training with frozen image encoders and large language models. *arXiv preprint arXiv:2301.12597*, 2023a.

Yifan Li, Yifan Du, Kun Zhou, Jinpeng Wang, Wayne Xin Zhao, and Ji-Rong Wen. Evaluating object hallucination in large vision-language models. *arXiv preprint arXiv:2305.10355*, 2023b.

Tsung-Yi Lin, Michael Maire, Serge Belongie, James Hays, Pietro Perona, Deva Ramanan, Piotr Dollár, and C Lawrence Zitnick. Microsoft coco: Common objects in context. In *Computer Vision–ECCV 2014: 13th European Conference, Zurich, Switzerland, September 6-12, 2014, Proceedings, Part V 13*, pp. 740–755. Springer, 2014.

Fangyu Liu, Guy Emerson, and Nigel Collier. Visual spatial reasoning. *Transactions of the Association for Computational Linguistics*, 11:635–651, 2023a.

Haotian Liu, Chunyuan Li, Qingyang Wu, and Yong Jae Lee. Visual instruction tuning. *arXiv preprint arXiv:2304.08485*, 2023b.

Shilong Liu, Zhaoyang Zeng, Tianhe Ren, Feng Li, Hao Zhang, Jie Yang, Chunyuan Li, Jianwei Yang, Hang Su, Jun Zhu, et al. Grounding dino: Marrying dino with grounded pre-training for open-set object detection. *arXiv preprint arXiv:2303.05499*, 2023c.

Pan Lu, Liang Qiu, Jiaqi Chen, Tony Xia, Yizhou Zhao, Wei Zhang, Zhou Yu, Xiaodan Liang, and Song-Chun Zhu. Iconqa: A new benchmark for abstract diagram understanding and visual language reasoning. *arXiv preprint arXiv:2110.13214*, 2021.

Junhua Mao, Jonathan Huang, Alexander Toshev, Oana Camburu, Alan L Yuille, and Kevin Murphy. Generation and comprehension of unambiguous object descriptions. In *Proceedings of the IEEE conference on computer vision and pattern recognition*, pp. 11–20, 2016.

Kenneth Marino, Mohammad Rastegari, Ali Farhadi, and Roozbeh Mottaghi. Ok-vqa: A visual question answering benchmark requiring external knowledge. In *Proceedings of the IEEE/cvf conference on computer vision and pattern recognition*, pp. 3195–3204, 2019.

Anand Mishra, Shashank Shekhar, Ajeet Kumar Singh, and Anirban Chakraborty. Ocr-vqa: Visual question answering by reading text in images. In *2019 international conference on document analysis and recognition (ICDAR)*, pp. 947–952. IEEE, 2019.

OpenAI. Introducing chatgpt. *https://openai.com/blog/chatgpt*, 2022.

Vicente Ordonez, Girish Kulkarni, and Tamara Berg. Im2text: Describing images using 1 million captioned photographs. *Advances in neural information processing systems*, 24, 2011.

Long Ouyang, Jeffrey Wu, Xu Jiang, Diogo Almeida, Carroll Wainwright, Pamela Mishkin, Chong Zhang, Sandhini Agarwal, Katarina Slama, Alex Ray, et al. Training language models to follow instructions with human feedback. *Advances in Neural Information Processing Systems*, 35:27730–27744, 2022.

Guilherme Penedo, Quentin Malartic, Daniel Hesslow, Ruxandra Cojocaru, Alessandro Cappelli, Hamza Alobeidli, Baptiste Pannier, Ebtesam Almazrouei, and Julien Launay. The refinedweb dataset for falcon llm: outperforming curated corpora with web data, and web data only. *arXiv preprint arXiv:2306.01116*, 2023.

Zhiliang Peng, Wenhui Wang, Li Dong, Yaru Hao, Shaohan Huang, Shuming Ma, and Furu Wei. Kosmos-2: Grounding multimodal large language models to the world. *arXiv preprint arXiv:2306.14824*, 2023.

Bryan A Plummer, Liwei Wang, Chris M Cervantes, Juan C Caicedo, Julia Hockenmaier, and Svetlana Lazebnik. Flickr30k entities: Collecting region-to-phrase correspondences for richer image-to-sentence models. In *Proceedings of the IEEE international conference on computer vision*, pp. 2641–2649, 2015.

Alec Radford, Jeffrey Wu, Rewon Child, David Luan, Dario Amodei, Ilya Sutskever, et al. Language models are unsupervised multitask learners. *OpenAI blog*, 1(8):9, 2019.

Jack W Rae, Sebastian Borgeaud, Trevor Cai, Katie Millican, Jordan Hoffmann, Francis Song, John Aslanides, Sarah Henderson, Roman Ring, Susannah Young, et al. Scaling language models: Methods, analysis & insights from training gopher. *arXiv preprint arXiv:2112.11446*, 2021.

Anna Rohrbach, Lisa Anne Hendricks, Kaylee Burns, Trevor Darrell, and Kate Saenko. Object hallucination in image captioning. *arXiv preprint arXiv:1809.02156*, 2018.

Teven Le Scao, Angela Fan, Christopher Akiki, Ellie Pavlick, Suzana Ilić, Daniel Hesslow, Roman Castagné, Alexandra Sasha Luccioni, François Yvon, Matthias Gallé, et al. Bloom: A 176b-parameter open-access multilingual language model. *arXiv preprint arXiv:2211.05100*, 2022.

Christoph Schuhmann, Richard Vencu, Romain Beaumont, Robert Kaczmarczyk, Clayton Mullis, Aarush Katta, Theo Coombes, Jenia Jitsev, and Aran Komatsuzaki. Laion-400m: Open dataset of clip-filtered 400 million image-text pairs. *arXiv preprint arXiv:2111.02114*, 2021.

Dustin Schwenk, Apoorv Khandelwal, Christopher Clark, Kenneth Marino, and Roozbeh Mottaghi. A-okvqa: A benchmark for visual question answering using world knowledge. In *European Conference on Computer Vision*, pp. 146–162. Springer, 2022.

Piyush Sharma, Nan Ding, Sebastian Goodman, and Radu Soricut. Conceptual captions: A cleaned, hypernymed, image alt-text dataset for automatic image captioning. In *Proceedings of the 56th Annual Meeting of the Association for Computational Linguistics (Volume 1: Long Papers)*, pp. 2556–2565, 2018.

Oleksii Sidorov, Ronghang Hu, Marcus Rohrbach, and Amanpreet Singh. Textcaps: a dataset for image captioningwith reading comprehension. 2020.

Amanpreet Singh, Vivek Natarajan, Meet Shah, Yu Jiang, Xinlei Chen, Dhruv Batra, Devi Parikh, and Marcus Rohrbach. Towards vqa models that can read. In *Proceedings of the IEEE/CVF conference on computer vision and pattern recognition*, pp. 8317–8326, 2019.

Shaden Smith, Mostofa Patwary, Brandon Norick, Patrick LeGresley, Samyam Rajbhandari, Jared Casper, Zhun Liu, Shrimai Prabhumoye, George Zerveas, Vijay Korthikanti, et al. Using deepspeed and megatron to train megatron-turing nlg 530b, a large-scale generative language model. *arXiv preprint arXiv:2201.11990*, 2022.

Rohan Taori, Ishaan Gulrajani, Tianyi Zhang, Yann Dubois, Xuechen Li, Carlos Guestrin, Percy Liang, and Tatsunori B. Hashimoto. Stanford alpaca: An instruction-following llama model. `https://github.com/tatsu-lab/stanford_alpaca`, 2023.

MosaicML NLP Team. Introducing mpt-7b: A new standard for open-source, commercially usable llms, 2023. URL `www.mosaicml.com/blog/mpt-7b`. Accessed: 2023-05-05.

Hugo Touvron, Thibaut Lavril, Gautier Izacard, Xavier Martinet, Marie-Anne Lachaux, Timothée Lacroix, Baptiste Rozière, Naman Goyal, Eric Hambro, Faisal Azhar, et al. Llama: Open and efficient foundation language models. *arXiv preprint arXiv:2302.13971*, 2023a.

Hugo Touvron, Louis Martin, Kevin Stone, Peter Albert, Amjad Almahairi, Yasmine Babaei, Nikolay Bashlykov, Soumya Batra, Prajjwal Bhargava, Shruti Bhosale, et al. Llama 2: Open foundation and fine-tuned chat models. *arXiv preprint arXiv:2307.09288*, 2023b.

Maria Tsimpoukelli, Jacob L Menick, Serkan Cabi, SM Eslami, Oriol Vinyals, and Felix Hill. Multimodal few-shot learning with frozen language models. *Advances in Neural Information Processing Systems*, 34: 200–212, 2021.

Peng Wang, An Yang, Rui Men, Junyang Lin, Shuai Bai, Zhikang Li, Jianxin Ma, Chang Zhou, Jingren Zhou, and Hongxia Yang. Ofa: Unifying architectures, tasks, and modalities through a simple sequence-to-sequence learning framework. In *International Conference on Machine Learning*, pp. 23318–23340. PMLR, 2022.

Wenhai Wang, Zhe Chen, Xiaokang Chen, Jiannan Wu, Xizhou Zhu, Gang Zeng, Ping Luo, Tong Lu, Jie Zhou, Yu Qiao, et al. Visionllm: Large language model is also an open-ended decoder for vision-centric tasks. *arXiv preprint arXiv:2305.11175*, 2023.

Bin Yan, Yi Jiang, Jiannan Wu, Dong Wang, Ping Luo, Zehuan Yuan, and Huchuan Lu. Universal instance perception as object discovery and retrieval. In *Proceedings of the IEEE/CVF Conference on Computer Vision and Pattern Recognition*, pp. 15325–15336, 2023.

Qinghao Ye, Haiyang Xu, Guohai Xu, Jiabo Ye, Ming Yan, Yiyang Zhou, Junyang Wang, Anwen Hu, Pengcheng Shi, Yaya Shi, et al. mplug-owl: Modularization empowers large language models with multimodality. *arXiv preprint arXiv:2304.14178*, 2023.

Licheng Yu, Patrick Poirson, Shan Yang, Alexander C Berg, and Tamara L Berg. Modeling context in referring expressions. In *Computer Vision–ECCV 2016: 14th European Conference, Amsterdam, The Netherlands, October 11-14, 2016, Proceedings, Part II 14*, pp. 69–85. Springer, 2016.

Susan Zhang, Stephen Roller, Naman Goyal, Mikel Artetxe, Moya Chen, Shuohui Chen, Christopher Dewan, Mona Diab, Xian Li, Xi Victoria Lin, et al. Opt: Open pre-trained transformer language models. *arXiv preprint arXiv:2205.01068*, 2022.

Deyao Zhu, Jun Chen, Kilichbek Haydarov, Xiaoqian Shen, Wenxuan Zhang, and Mohamed Elhoseiny. Chatgpt asks, blip-2 answers: Automatic questioning towards enriched visual descriptions. *arXiv preprint arXiv:2303.06594*, 2023a.

Deyao Zhu, Jun Chen, Xiaoqian Shen, Xiang Li, and Mohamed Elhoseiny. Minigpt-4: Enhancing vision-language understanding with advanced large language models. *arXiv preprint arXiv:2304.10592*, 2023b.

Mingchen Zhuge, Haozhe Liu, Francesco Faccio, Dylan R Ashley, Róbert Csordás, Anand Gopalakrishnan, Abdullah Hamdi, Hasan Abed Al Kader Hammoud, Vincent Herrmann, Kazuki Irie, et al. Mindstorms in natural language-based societies of mind. *arXiv preprint arXiv:2305.17066*, 2023.

A Appendix

In the supplementary, we provide more qualitative results that are generated from our model to demonstrate the vision-language multi-tasking capabilities.

A.1 Instruction template for various vision-language tasks

RefCOCO/RefCOCO+/RefCOCOg: *[refer] give me the location of question*

VizWiz: *[vqa] Based on the image, respond to this question with a single word or phrase: question, and reply 'unanswerable' when the provided information is insufficient*

Hateful Meme: *[vqa] This is an image with: question written on it. Is it hateful? Answer:*

VSR: *[vqa] Based on the image, is this statement true or false? question*

IconQA, GQA, OKVQA: *[vqa] Based on the image, respond to this question with a single word or phrase: question*

A.2 Additional Qualitative Results

To study how well our model is able to take visual input and answer questions based on task-oriented identifier, we use our model to perform multiple vision-language tasks including grounded image captioning in Fig. 4, Fig. 5, Fig. 6 and Fig. 7; Object parsing and grounding in Fig. 8, Fig. 9, Fig. 10 and Fig. 11; Referring expression comprehension in Fig. 12, Fig. 13, Fig. 14 and Fig. 15; Object identification in Fig. 16, Fig. 17, Fig. 18 and Fig. 19.

For each task, we share 4 examples for showing the vision-language capabilities of our model. The results in the demo provide direct evidence for the competing visual understanding capabilities of MiniGPT-v2 on multiple vision-language tasks. For example, in the cases of grounded caption, our model is able to give correct grounded image caption with detailed spatial locations of objects. In the cases of identify, the model also generates our expected object names. MiniGPT-v2 can understand the new scenes and follow the question identifier to respond. But we also need to note that our model still has some hallucination e.g., In Fig. 6, several persons are not grounded accurately, and in Fig. 7, there does not exist a vase in the image.

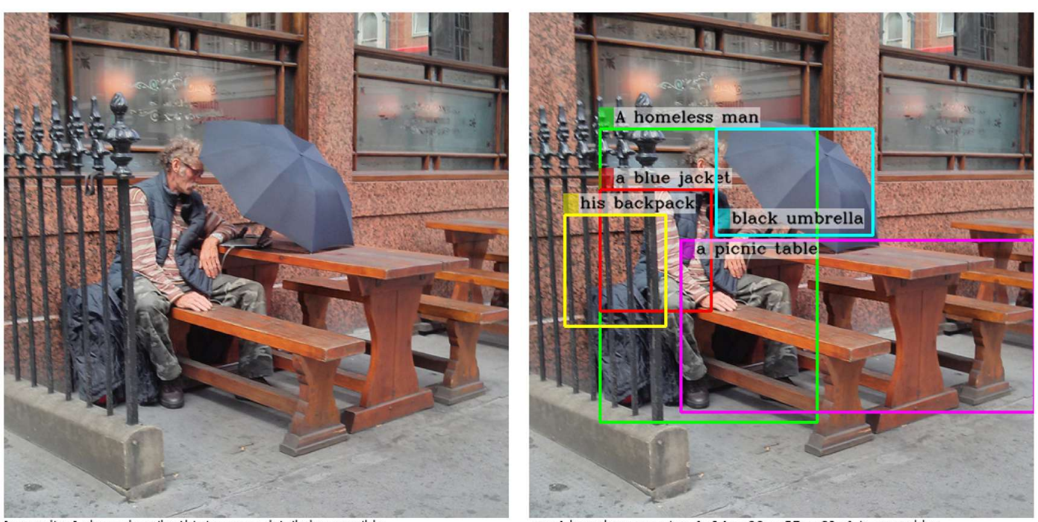

Figure 4: Detail grounded image caption example.

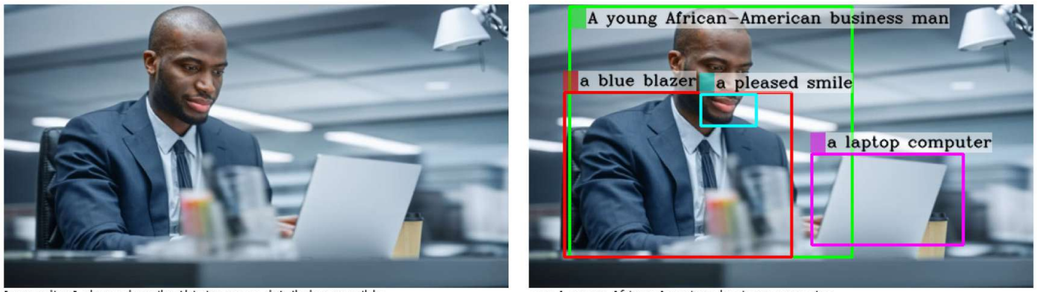

[grounding] please describe this image as detailed as possible

<p>A young African-American business man</p>
{<8><1><64><89>} in <p>a blue blazer</p>
{<7><31><52><89>} looks up at the camera with <p>a
pleased smile</p> {<34><32><45><43>} while working at
his desk, using <p>a laptop computer</p>

Figure 5: Detail grounded image caption example

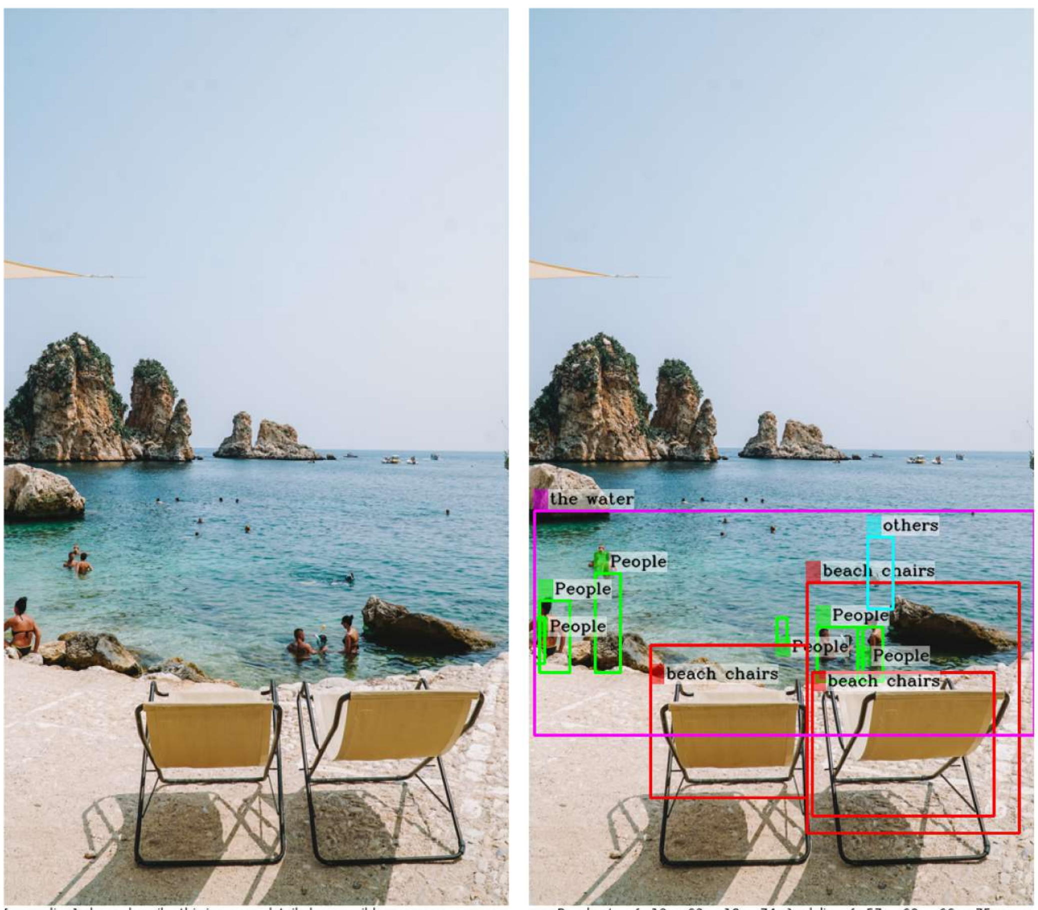

[grounding] please describe this image as detailed as possible

<p>People</p> {<13><63><18><74>}<delim>{<57><69><66><75
>}<delim>{<2><66><8><74>}<delim>{<65><69><70><75>}<deli
m>{<1><68><3><73>}<delim>{<49><68><51><71>} sit and lay
on <p>beach chairs</p> {<55><64><97><92>}<delim>{<24><7
1><55><88>}<delim>{<56><74><92><90>} while

Figure 6: Detail grounded image caption example

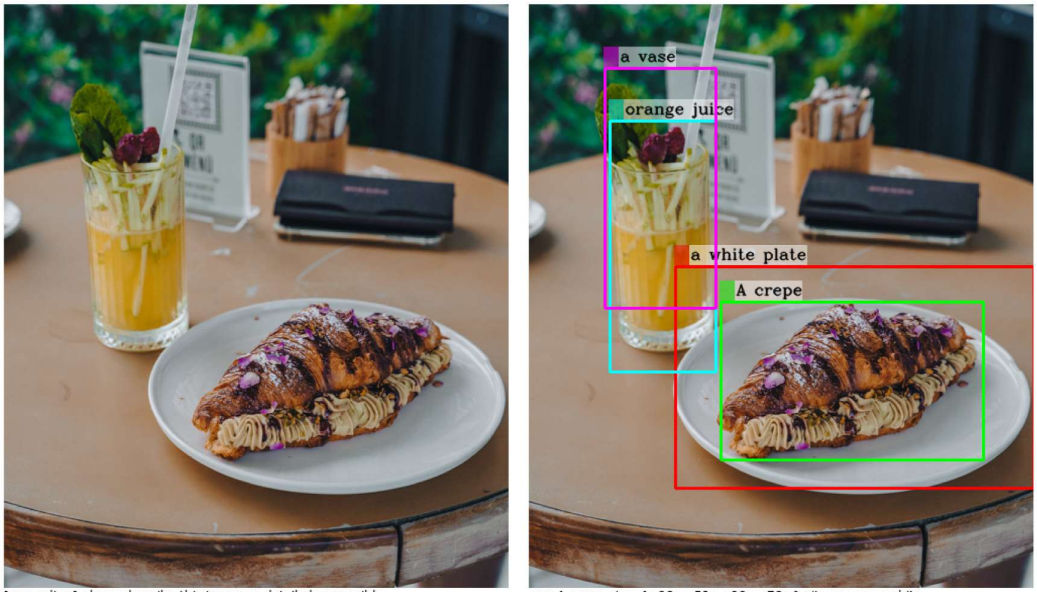

[grounding] please describe this image as detailed as possible

<p>A crepe</p> {<38><51><90><78>} sits on <p>a white plate</p> {<29><45><100><83>} near a cup of <p>orange juice</p> {<16><20><37><63>} and <p>a vase</p> {<15><11><37><52>} with a stem in the background .

Figure 7: Detail grounded image caption example

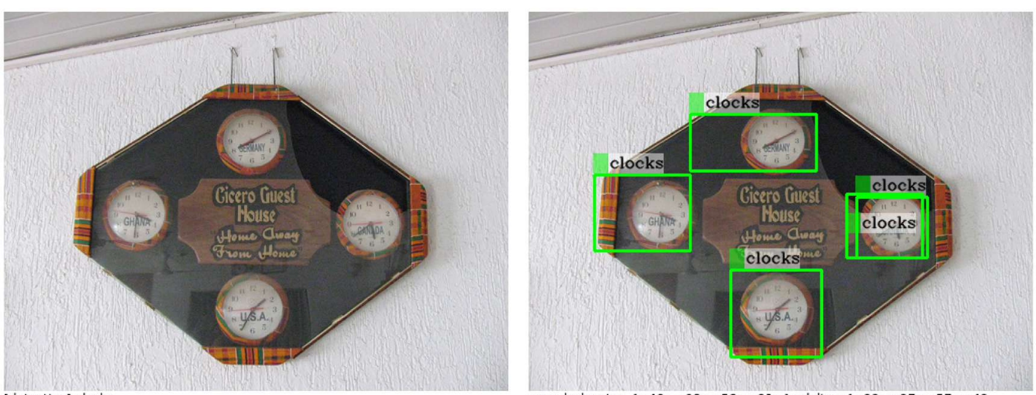

[detection] clocks

<p>clocks</p> {<40><68><58><91>}<delim>{<32><27><57><42 >}<delim>{<13><43><32><63>}<delim>{<65><49><79><65>}<de lim>{<63><48><78><65>}

Figure 8: Object parsing and grounding example

Figure 9: Object parsing and grounding example

Figure 10: Object parsing and grounding example

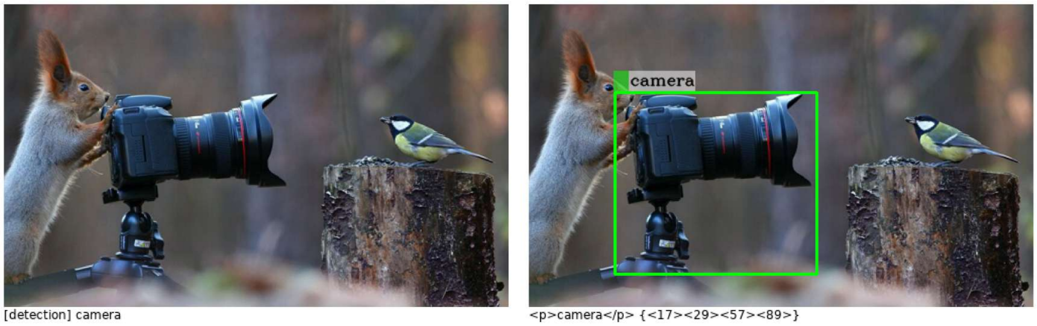

Figure 11: Object parsing and grounding example

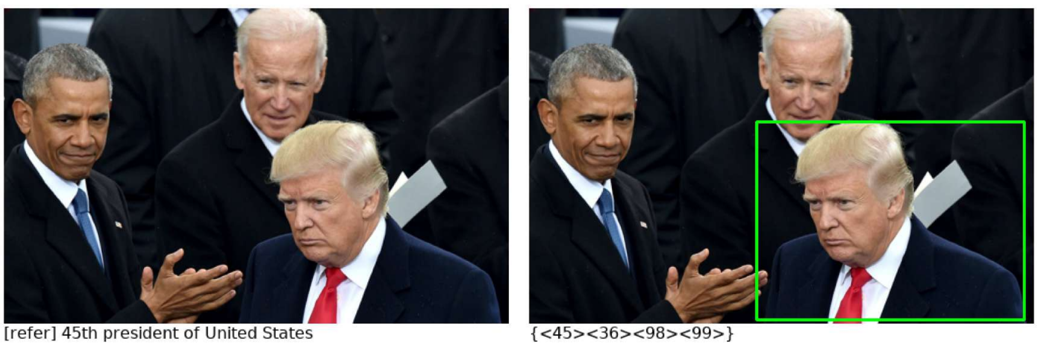

Figure 12: Referring expression comprehension example

Figure 13: Referring expression comprehension example

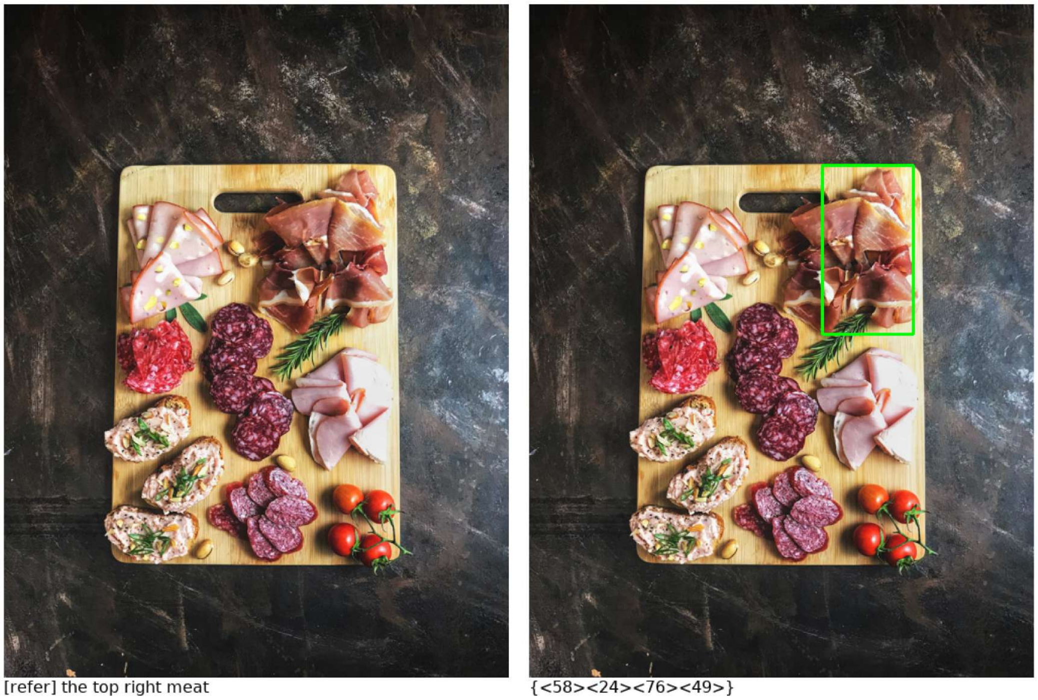

Figure 14: Referring expression comprehension example

Figure 15: Referring expression comprehension example

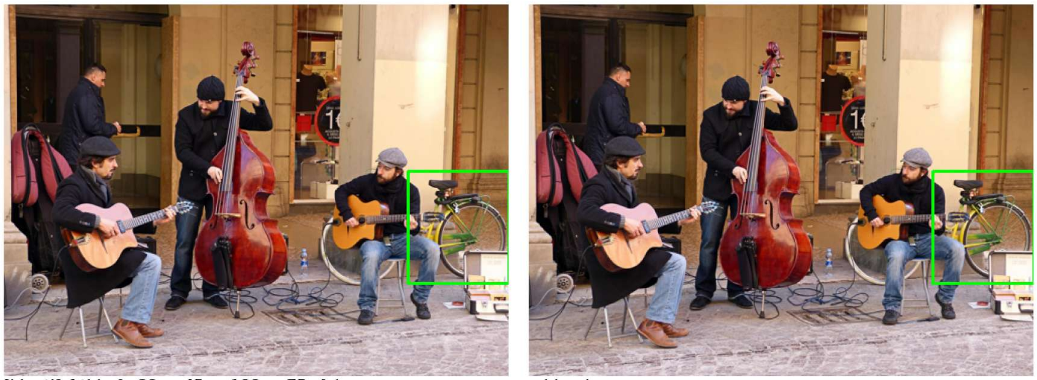

Figure 16: object identification example

Figure 17: object identification example

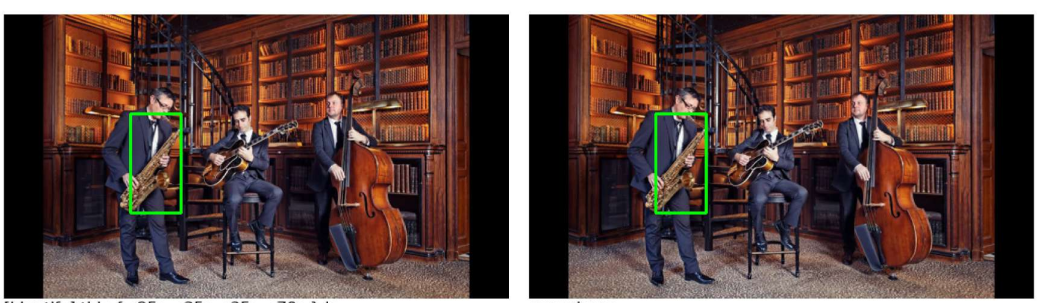

Figure 18: object identification example

Figure 19: object identification example